C. R. Chimie 21 (2018) 993–1000

Contents lists available at ScienceDirect

Comptes Rendus Chimie

www.sciencedirect.com

Full paper/Mémoire

Ultraquick synthesis of hydrotalcite-like compounds as efficient catalysts for the oxidation of volatile organic compounds

Synthèse ultra-rapide de matériaux dérivés des composés de type hydrotalcite comme catalyseurs efficaces pour l'oxydation des composés organiques volatils

Cynthia Abou Serhal [a, b], Isabelle Mallard [a], Christophe Poupin [a], Madona Labaki [b], Stéphane Siffert [a, *], Renaud Cousin [a, **]

[a] *Université du Littoral Côte d'Opale (ULCO), Unité de chimie environnementale et interactions sur le vivant (UCEIV, E.A. 4492), MREI, 59140 Dunkerque, France*

[b] *Lebanese University, Laboratory of Physical Chemistry of Materials (LCPM)/PR2N, Faculty of Sciences, Fanar, P.O. Box 90656, Jdeidet El Metn, Lebanon*

ARTICLE INFO

Article history:
Received 25 July 2018
Accepted 17 September 2018
Available online 20 October 2018

Keywords:
Cobalt oxide
Hydrotalcite
Microwave irradiation
Mixed oxides
Propene oxidation

ABSTRACT

To improve the physicochemical properties and the catalytic activities of hydrotalcite materials toward the total oxidation of volatile organic compounds, microwave irradiations were used as a nonconventional treatment. Several Mg-Co/Al-Fe layered double hydroxides with a molar ratio $M^{2+}/M^{3+} = 2$ were synthesized and evaluated as catalyst precursors toward propene oxidation. In this study, very efficient catalysts were prepared using low microwave power during short irradiation time (40 W, 1 min) as compared with usual microwave parameters.

Mots-clés:
Oxyde de cobalt
Hydrotalcite
Irradiation micro-ondes
Oxydes mixtes
Oxydation du propène

RÉSUMÉ

Afin d'améliorer les propriétés physicochimiques et les activités catalytiques des matériaux hydrotalcite vis-à-vis de l'oxydation totale des composés organiques volatils (COV), des irradiations micro-ondes ont été utilisées comme traitement non conventionnel lors de la synthèse de ces matériaux. Une série d'oxydes mixtes Mg-Co/Al-Fe dérivée des composés hydrotalcites avec un rapport molaire $M^{2+}/M^{3+} = 2$ a été synthétisée et évaluée en tant que précurseurs de catalyseurs vis-à-vis de l'oxydation du propène. Dans ce travail, des catalyseurs très efficaces ont été préparés en utilisant des rayonnements micro-ondes avec

* Corresponding author.
** Corresponding author.
E-mail addresses: stephane.siffert@univ-littoral.fr (S. Siffert), renaud.cousin@univ-littoral.fr (R. Cousin).

https://doi.org/10.1016/j.crci.2018.09.012

une faible puissance pendant un temps d'irradiation court (40 W, 1 min) comparé aux paramètres micro-ondes normalement utilisés.

1. Introduction

The catalytic oxidation of volatile organic compounds (VOCs) into less toxic byproducts is one of the most efficient methods to eliminate the emissions of these harmful pollutants. The catalysts used in our study are prepared by hydrotalcite route. Hydrotalcite-like compound with the general formula $[M(II)_{1-x}M(III)_x(OH)_2]^{x+}(A^{n-})_{x/n}\cdot yH_2O$ consists of brucite-like layers $Mg(OH)_2$, in which a part of the divalent cations M(II) is substituted by trivalent cations M(III). The nature of the cations can be changed in a broad range. Divalent and trivalent metals having an ionic radius between 65 and 80 pm (Ni^{2+}, Co^{2+}, Zn^{2+}, etc.) and 50 and 69 pm (Al^{3+}, Fe^{3+}, etc.), respectively, can lead to the formation of hydrotalcite-like compounds. Each cation is located in the center of an octahedron and surrounded by six hydroxyl groups (OH^-). The positive charge (x^+) resulting from this replacement is balanced by anions (A^{n-}) (most commonly carbonate) and water molecules, located in interlayer domains [1].

Usually, hydrotalcite-like compounds are obtained by the traditional coprecipitation method requiring a long maturation phase [2–4]. Several new synthesis methods have been developed in the aim to improve hydrotalcites textural and structural properties [5] especially microwave irradiation. In fact, this method is mainly used for accelerating organic reactions and synthesizing inorganic solids [5,6]. Interestingly, Benito et al. [8] showed that microwave treatment at 125 °C leads to a significant improvement in hydrotalcite synthesis method not only by reducing the crystallization time but also by enhancing their physicochemical properties such as particle size. At the same time, they also demonstrated the full reconstruction of hydrotalcite catalyst by using microwave irradiation at various temperatures and reaction times (from 100 to 175 °C and 10–300 min, respectively) [9]. Moreover, catalysts aged under microwave give better catalytic performances toward styrene oxide hydrogenation to obtain 2-phenylethanol [9] driven by a better metal dispersion, as compared with conventional heating. In addition, the increase in aging time, temperature, and power (600 W) favors the crystallinity and the homogeneity of prepared materials [10,11].

Previously, we have reported that oxides prepared via the hydrotalcite route using microwave irradiations at 80 °C for 1 h (300 W) exhibited an interesting catalytic performance for the oxidation of toluene [12].

The purpose of this article is to successfully synthesize hydrotalcite-like materials using microwave irradiation for a short time. The challenge of this study is also to avoid the high temperature and power and to enhance the efficiency of the calcined catalysts toward VOC oxidation.

2. Experimental section

2.1. Catalyst synthesis

Several hydrotalcite-like samples with a molar ratio $M^{2+}/M^{3+} = 2$ were synthesized by coprecipitation method. A nitrate aqueous solution containing the appropriate dissolved amount of $Mg(NO_3)_2\cdot 3H_2O$ (Acros Organics, 99%), $Co(NO_3)_2\cdot 3H_2O$ (Chem-Lab, 97%), $Al(NO_3)_3\cdot 9H_2O$ (Chem-Lab, 98.5%), and $Fe(NO_3)_3\cdot 9H_2O$ (Chem-Lab, 98%) was added dropwise at room temperature into a stirred 1 M sodium carbonate (Acros, 99.5%) solution. The pH was fixed and maintained at 10 using 2 M sodium hydroxide (Panreac, 98%) solution. After complete precipitation of the mixture, a part of the slurry was kept 24 h under vigorous stirring to obtain the hydrotalcite structure. Another part of the precipitate was submitted to a microwave treatment where power and duration were maintained fixed at 40 W and 1 min, respectively, using a Biotage cavity microwave oven. The maximum heating temperature reached during this treatment was only a room temperature of 33 °C.

Finally, all samples were filtered, washed with hot deionized water until neutralization, and dried for 48 h. The obtained precipitates were ground and calcined under an air flow (2 L h^{-1}, 1 °C min^{-1}) at 500 °C for 4 h. Uncalcined samples will be denoted by $M(II)_4M(III)_2$-CT and $M(II)_4M(III)_2$-MW, where CT and MW represent the conventional and microwave treatment, respectively, whereas M(II) and M(III) represent the divalent and trivalent cations. The subscripts represent the molar ratio of each metal. The samples calcined at 500 °C will be designated as $M(II)_4M(III)_2$-CT500 and $M(II)_4M(III)_2$-MW500.

For catalytic comparison purposes, Co_4Fe_2 samples were also prepared using microwave irradiations at a fixed power of 40 W for 45 and 10 s. The as-prepared samples will be denoted by Co_4Fe_2-MW500-45sec and Co_4Fe_2-MW500-10sec, respectively. In addition, a commercial 0.5 wt% Pd/Al_2O_3 (Acros Organics) was also used for comparison purpose.

2.2. Characterization techniques

The elemental composition of the samples was analyzed using an inductively coupled plasma (ICP) optical emission spectrometer (Thermo ICAP 6300 DUO). Structural analysis of the different catalysts was carried out at room temperature by X-Ray diffraction (XRD) technique using a Bruker D8 Advance diffractometer, with a copper anode Cu Kα radiation. A count time of 2 s per step with a resolution of 0.02° was used. Identification of the crystalline phases was made with the Joint Committee on Powder Diffraction Standards (JCPDS) files, using EVA software from Bruker. The specific

surface area was calculated by the Brunauer–Emmett–Teller (BET) method, by nitrogen adsorption at low temperature (−196 °C), using an Ankersmit Quanta Sorb Junior apparatus. Before the adsorption, the uncalcined samples were degassed at 60 °C for 45 min and the calcined samples at 130 °C for 30 min. Pore diameters and pore volumes were determined by Barrett–Joyner–Halenda method, using a Sorptomatic 1990 sorption analyzer. Before the measurements, each calcined sample was degassed at 400 °C for 5 h. H_2-temperature programmed reduction (H_2-TPR) was also carried out on the calcined samples. Hydrogen consumption was detected by a thermal conductivity detector using an Altamira AMI 200 apparatus. Sample (12 mg) was heated from room temperature to 950 °C (5 °C min^{-1}) in a 5 vol % of H_2/Ar, with a total gas flow of 30 mL min^{-1}. Field-emission scanning electron microscopy (SEM) was obtained using JSM-711F equipment, with an accelerating voltage of 15 kV. Powder catalysts were adhered on carbon adhesive and coated with a 10-nm chrome film.

2.3. Catalytic test

Catalytic performance of each sample was evaluated toward the total oxidation of propene, at atmospheric pressure. Each catalyst (100 mg) was loaded into a fixed bed reactor and pretreated under an airflow at 150 °C for 30 min. The oxidation test was carried out from 150 to 500 °C (1 °C min^{-1}) under a total flow rate of 100 mL min^{-1} containing 6000 ppm of propene in air balance. The reactants and the oxidation products were then analyzed using a Varian CP-4900 Micro–Gas Chromatograph.

Catalytic activities were evaluated at 20 % of propene conversion:

$$A = \frac{Q \times 273.15 \times [C_3H_6]_0 \times X}{V_M \times T_{20} \times 10^6 \times m}$$

where A is the catalytic activity (mol h^{-1} g^{-1}), Q is the volume flow (L h^{-1}), V_M is the molar volume (L mol^{-1}), T_{20} is the catalysts temperature for 20 % propene conversion (K), $[C_3H_6]_0$ is the propene initial concentration (ppm), and X is the propene conversion (%); and M is the catalyst mass (g).

3. Results and discussion

3.1. Characterization

The ICP results presented in Table 1 show that experimental molar ratio M^{2+}/M^{3+} is in a good agreement with the theoretical value. For Co_4Fe_2 and Co_4Al_2 samples, the experimental molar ratio is slightly greater than 2, whereas for Mg_4Fe_2 and Mg_4Al_2 samples it is slightly lower.

X-ray diffractograms of the uncalcined samples prepared by the conventional and microwave irradiations are presented in Fig. 1. The patterns obtained correspond to the rhombohedral hydrotalcite phase. It should be noted that the intensities of the diffraction peaks differ with the substitution of the divalent magnesium cation with cobalt and the trivalent aluminum cation by iron. Thus, the introduction of cobalt or iron decreases the crystallinity of the synthesized hydrotalcite material. However, for the Mg_4Al_2-MW sample, a second crystalline compound was identified and corresponds to the $Al(OH)_3$ gibbsite phase. The formation of the $Al(OH)_3$ gibbsite could be explained by the lowest molar Mg/Al ratio obtained for Mg_4Al_2-MW sample in ICP. Moreover, for the cobalt-containing samples, a small shoulder was detected at approximately $22\theta = 33.5°$, assigned to the minor phase of cobalt hydroxide α-$Co(OH)_2$. This appearance is not related to microwave irradiation treatment, because it is also detected on the samples prepared by the conventional synthesis. This phase was also detected by Gennequin et al. [13] for hydrotalcite-like compound with high cobalt content.

Table 1 summarizes the values of the crystallographic parameters of the dried solids, determined by XRD measurements, using Miller indices. In fact, parameter a indicates the average cation–cation distance located in the layers, whereas the c parameter is related to the thickness of the interlayer domain [14]. Thereby, the cell parameter a increases proportionally to the ionic radius of the cations located in the octahedron center, for example, when Al^{3+} is substituted by Fe^{3+}. It should be noted that, microwave irradiation has no effect on a values, indicating that brucite-like layers are not modified with the microwave exposure [8].

There is a decrease in the c parameter after microwave irradiation treatment, especially for the magnesium-containing samples suggesting a decrease in the molar ratio $M^{2+}/M^{3+} = 2$, leading to a higher aluminum content [3,15]. Indeed, the presence of gibbsite phase detected by XRD can be attributed to the excess of aluminum that has not been incorporated in the hydrotalcite network. This result highlights the correlation between c parameter and the basal spacing, indicating stronger electrostatic interactions [8,16]. A significant reduction in crystallite sizes was obtained for Mg_4Al_2-MW and for Co_4Fe_2-MW, both of

Table 1
Chemical analysis, cell parameters, and specific surface areas of the uncalcined samples.

Samples	Chemical analysis		c (Å)	a (Å)	Crystallite size (nm)	Specific surface area (m^2 g^{-1})
	Theoretical	Experimental				
Mg_4Al_2-CT	2	1.95	23.3	3.04	13.1	99
Mg_4Al_2-MW	2	1.5	22.8	3.04	5.9	128
Mg_4Fe_2-CT	2	1.96	23.6	3.12	12.8	90
Mg_4Fe_2-MW	2	1.92	23	3.10	12.7	100
Co_4Al_2-CT	2	2.12	22.5	3.06	16.6	52
Co_4Al_2-MW	2	2.24	22.4	3.06	16.5	63
Co_4Fe_2-CT	2	2.05	22.7	3.12	17	68
Co_4Fe_2-MW	2	2.04	22.4	3.12	11.9	91

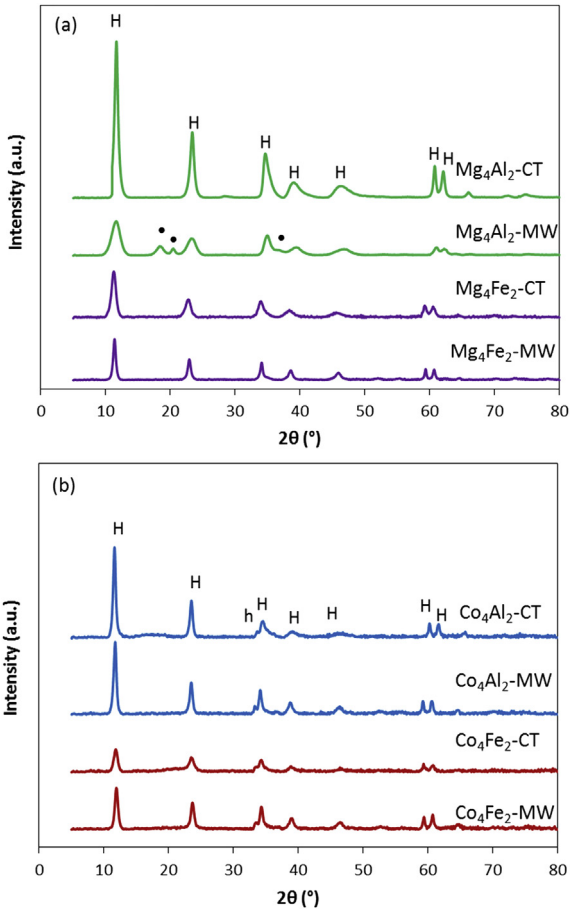

Fig. 1. XRD patterns of the uncalcined samples: (a) Mg_4Al_2 and Mg_4Fe_2 and (b) Co_4Al_2 and Co_4Fe_2. H, hydrotalcite phase (JCPDS No. 22-0700); •, $Al(OH)_3$ gibbsite phase (JCPDS No. 33-0018); h, cobalt hydroxide α-$Co(OH)_2$ (JCPDS No. 46-0605).

them exhibiting a weaker crystallization as compared with the conventional synthesis.

Dried samples prepared via the conventional route have specific surface areas comprised between 50 and 100 $m^2\ g^{-1}$ whereas the surface area increased for all microwave treated samples (Table 1). The best results were obtained for microwave Mg_4Al_2, Mg_4Fe_2, and Co_4Fe_2 catalysts and can be explained by an increase in the number of crystallites formed, giving rise to small dispersed particles and thus to lower aggregation [8,17]. In fact, microwave irradiation accelerates the heating process by reducing the thermal gradient between the bulk and the surface [18] and therefore the crystallite formation, and enhances the nucleation, giving higher specific surface areas.

The XRD patterns of the calcined samples treated under microwave are presented in Fig. 2. The absence of characteristic peaks of the hydrotalcite-like structure for all calcined samples was noted. Therefore, a destruction of this phase has occurred after thermal treatment at 500 °C, and new crystalline phases were obtained instead [19]. From these results, it can be seen that the hydrotalcite structure was transformed into mixed oxides of the divalent and trivalent cations present. However, it is hard to detect each

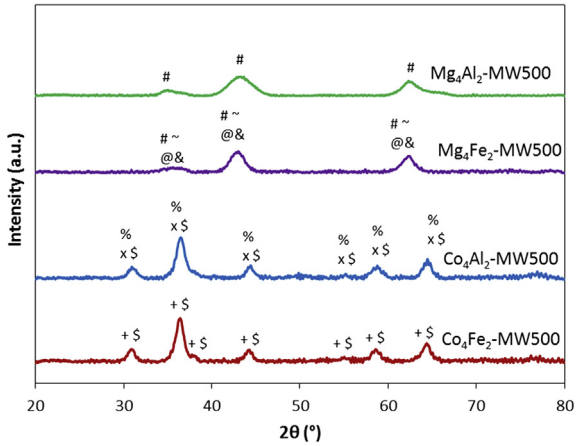

Fig. 2. XRD patterns of the calcined samples treated under microwave. #, MgO (JCPDS No. 45-0946); ~, Fe_3O_4 (JCPDS No. 89-0691); @, γ-Fe_2O_3 (JCPDS No. 04-0755); and &, $MgFe_2O_4$ (JCPDS No. 36-0398); %, Co_2AlO_4 (JCPDS No. 38-0814); X, $CoAl_2O_4$ (JCPDS No. 44-0160); $, Co_3O_4 (JCPDS No. 42-1467); and +, $CoFe_2O_4$ (JCPDS No. 22-1086).

oxide separately because of the same 2θ values and the similar relative intensities of the diffraction lines. For Mg_4Al_2-CT500 and Mg_4Al_2-MW500 catalysts, the only phase detected was MgO periclase. For the other synthesized solids, the $A(III)B_2(II)O_4$ spinel-type oxides and M_3O_4 oxides are detected. When aluminum is replaced by iron in Mg_4Fe_2-CT500 and Mg_4Fe_2-MW500 catalysts, Fe_3O_4, γ-Fe_2O_3, or/and $MgFe_2O_4$ phases appeared. For cobalt-containing solids, Co_2AlO_4, $CoAl_2O_4$, or/and Co_3O_4 phases are identified for the Co_4Al_2-CT500 and Co_4Al_2-MW500 catalysts. However, for Co_4Fe_2-CT500 and Co_4Fe_2-MW500 samples, the $CoFe_2O_4$ or/and Co_3O_4 phases were detected.

The isotherms obtained for all samples (shown in Supplementary Information) are of type IV, based on the IUPAC classification, attributed to mesoporous materials, with the exception of the catalyst Mg_4Al_2-MW. The latter is of type II corresponding to macroporous materials. Solids resulting from both syntheses present a hysteresis loop of type H1 with a "plateau" at high P/P_0 often associated with agglomerates that result in a narrow pore size distribution. On the contrary, for Mg_4Al_2-MW solid, the shape of the hysteresis loop differs after microwave treatment and changes to type H3, corresponding to aggregates generating nonuniform-sized slit pores [7].

Moreover, there is a clear change in the pore size distribution and in the pore volume (Table 2). Treating the solids with microwave irradiation increased the average pore diameter of all samples. Indeed, this observation is more pronounced for the Mg_4Al_2 catalyst. The solid Mg_4Al_2-CT500 resulting from the conventional route exhibits a narrow distribution of pores around 17 nm. In contrast, the average pore diameter of the same solid treated with microwave irradiations at 40 W has significantly increased to a range of 83 nm, corresponding to macroporous materials. In addition, an increase in the values of the specific surface areas is observed when the solids were calcined at 500 °C. This increase can be explained by the passage from a crystallized structure of

Table 2
Pore diameter, pore volume, specific surface areas, and temperature of 50 % of propene conversion (T_{50}) of the oxide catalysts.

Samples	Pore diameter (nm)	Pore volume ($cm^3\ g^{-1}$)	Specific surface area ($m^2\ g^{-1}$)	H_2 consumption ($\mu mol\ g^{-1}$)	T_{50} (°C)
Mg_4Al_2-CT500	17	0.9	236	n.d.[a]	>500
Mg_4Al_2-MW500	84	1.3	260	n.d.[a]	398
Mg_4Fe_2-CT500	14	0.5	127	5535	370
Mg_4Fe_2-MW500	22	0.6	130	5656	356
Co_4Al_2-CT500	23	0.5	73	12,380	261
Co_4Al_2-MW500	26	0.7	144	12,465	233
Co_4Fe_2-CT500	19	0.3	57	16,622	244
Co_4Fe_2-MW500	26	0.2	80	18,329	214

[a] Not determined.

hydrotalcite type to a mixed oxide type structure as already confirmed with the XRD analysis. The departure of water and carbonates results in the creation of craters in the samples [10]. Higher specific surface areas are obtained for the samples treated under microwave irradiations as compared with their homologous. In addition, this increase and in particular for Mg_4Al_2 solid can also be ascribed to the significant increase in the pore volume after microwave irradiations. However, the low difference in specific surface area between Mg_4Fe_2-CT500 and Mg_4Fe_2-MW500 can be considered within the experimental error of the BET measurement.

The Mars–van Krevelen mechanism is generally proposed for the VOC oxidation. It is then important to investigate the redox behavior of the catalysts and to study the reducibility of the species present in each catalyst. For comparison purposes, pure oxides of Fe_2O_3, Co_3O_4, and a mixture of both oxides ($Fe_2O_3 + Co_3O_4$) in the same ratio as in our samples were used. The consumption of hydrogen is reported in Table 2. The TPR profiles of all calcined samples are presented in Fig. 3. For the Mg_4Al_2 samples (not shown in the graph), no peaks were detected, indicating that the magnesium and aluminum oxides were not reduced in the studied temperature range and under the experimental conditions used. Pure Fe_2O_3 oxides (Fig. 3(a)) are reduced to Fe_3O_4 at temperatures between 370 and 450 °C and then Fe_3O_4 is reduced to FeO and Fe species [20,21], at 530 and 612 °C, according to the following equations:

$$3Fe_2O_3 + H_2 \rightarrow 2Fe_3O_4 + H_2O \quad (1)$$

$$Fe_3O_4 + H_2 \rightarrow 3FeO + H_2O \quad (2)$$

$$FeO + H_2 \rightarrow Fe + H_2O \quad (3)$$

Regarding the Mg_4Fe_2-CT500 catalyst, XRD has shown that iron can be present in the forms of γ-Fe_2O_3 and $MgFe_2O_4$. The reduction peaks were shifted to lower temperatures at 340 °C (Fe_2O_3 to Fe_3O_4) and 485 °C (Fe_3O_4 to FeO). In addition, the catalyst Mg_4Fe_2-MW500 treated under microwave irradiations shows three reduction peaks, a first reduction at lower temperature of 315 °C (Fe_2O_3 to Fe_3O_4), a second at 386 °C (Fe_3O_4 to FeO), and a wide at around 510 °C (FeO to Fe or/and to the reduction of $MgFe_2O_4$).

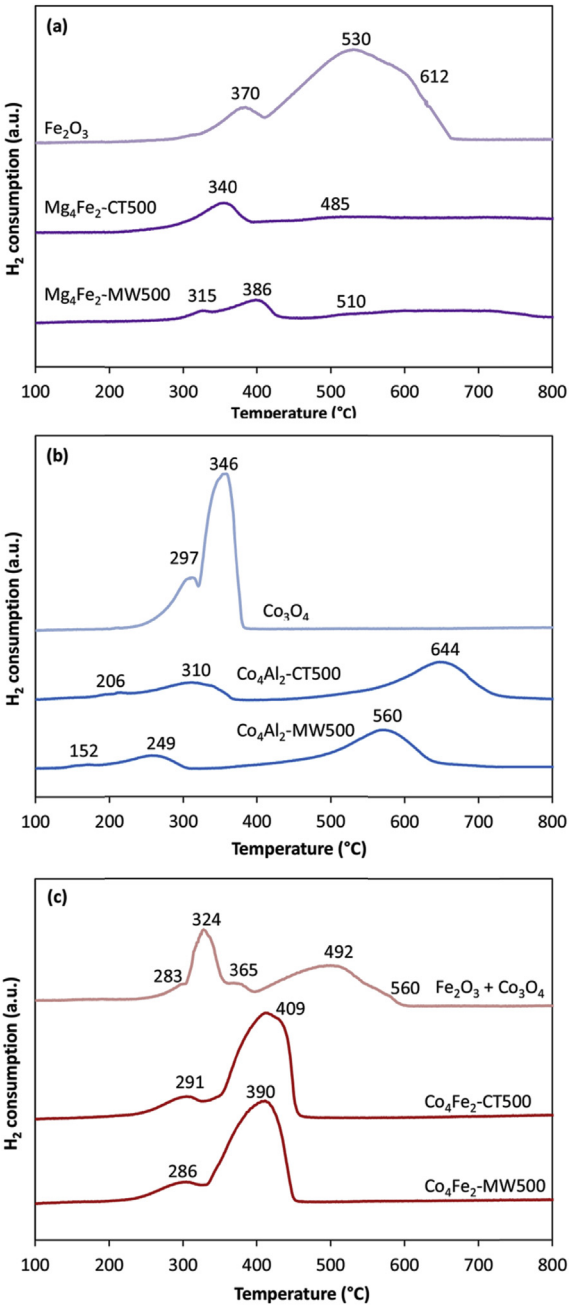

Fig. 3. TPR profiles of the calcined samples: (a) Fe_2O_3 and Mg_4Fe_2; (b) Co_3O_4 and Co_4Al_2; and (c) $Fe_2O_3 + Co_3O_4$ and Co_4Fe_2.

On the other hand, pure Co_3O_4 (Fig. 3(b)) exhibited two major reduction peaks centered at 297 and 346 °C. According to the literature [22,23], Co_3O_4 is reduced in two stages as shown in the following two equations:

$$Co_3O_4 + H_2 \rightarrow 3CoO + H_2O \quad (4)$$

$$3CoO + 3H_2 \rightarrow 3Co + 3H_2O \quad (5)$$

TPR profiles of Co/Al-containing catalysts prepared by the conventional and microwave methods (Co_4Al_2-CT500 and Co_4Al_2-MW500) show two peaks at low temperature (<350 °C) because of the reduction of Co_3O_4 into CoO and Co. The first peak is at 206 and 152 °C and the second peak is at 310 and 249 °C for Co_4Al_2-CT500 and Co_4Al_2-MW500, respectively. The peak detected at higher temperature for both solids corresponds to the reduction of Co_2AlO_4 to Co [12] (Eqs. 6–8). This peak is also shifted to lower temperature from 644 to 560 °C, when a conventional synthesis method was performed under microwave irradiations.

$$2Co_2AlO_4 + H_2 \rightarrow CoAl_2O_4 + 3CoO + H_2O \quad (6)$$

$$CoAl_2O_4 + 3CoO + 4H_2 \rightarrow 4Co + Al_2O_3 + 4H_2O \quad (7)$$

$$CoAl_2O_4 + H_2 \rightarrow Co + Al_2O_3 + H_2O \quad (8)$$

For the cobalt iron–based catalysts (Co_4Fe_2-CT500 and Co_4Fe_2-MW500) in Fig. 3(c), other than the Co_3O_4 oxides, XRD revealed the presence of $CoFe_2O_4$ species that were reduced at higher temperature (Eqs. 9 and 10). Moreover, it is clear that with Co_4Fe_2-CT500, the peak at high reduction temperature has a more intense area and has shifted toward lower reduction temperature than the Co_4Al_2-CT500 solid. This could be explained by the fact that iron oxides Fe_2O_3 are reduced simultaneously with cobalt oxides according to Eqs. 1–3. Indeed, the decrease in temperature is due to the increase in species that are likely to be reduced. The reduction of active cobalt species was enhanced by the presence of iron that has accelerated the reduction and therefore decreased the maximum reduction temperature from 644 to 409 °C.

$$CoFe_2O_4 + H_2 \rightarrow Co + Fe_2O_3 + H_2O \quad (9)$$

$$3Fe_2O_3 + H_2 \rightarrow 2Fe_3O_4 + H_2O \quad (10)$$

It is to be noted that the microwave treated samples present reduction peaks at lower temperature than the conventional treated samples. Furthermore, it is evident from Table 2 that irradiating a sample by microwave led to an increase in the amount of reducible species. This fact could be correlated with the higher surface areas and higher pore volumes obtained for the microwave-irradiated samples, which facilitate the accessibility of hydrogen.

From the SEM images of the Co_4Fe_2 catalysts presented in Fig. 4, a clear change in morphology is observed between samples prepared with or without microwave irradiation. Concerning the dried sample, Co_4Fe_2-CT shows well-defined layers, typical for the hydrotalcite structure. However, for Co_4Fe_2-MW catalyst, the layer morphology revealed a more open structure. After calcination, the SEM images show that Co_4Fe_2-CT500 is composed of clusters and large particles, unlike Co_4Fe_2-MW500 catalyst, whose images shown in Fig. 4 evidence the existence of smaller and more uniform particle size, in the origin of the increase in the surface area of samples treated under microwave irradiation.

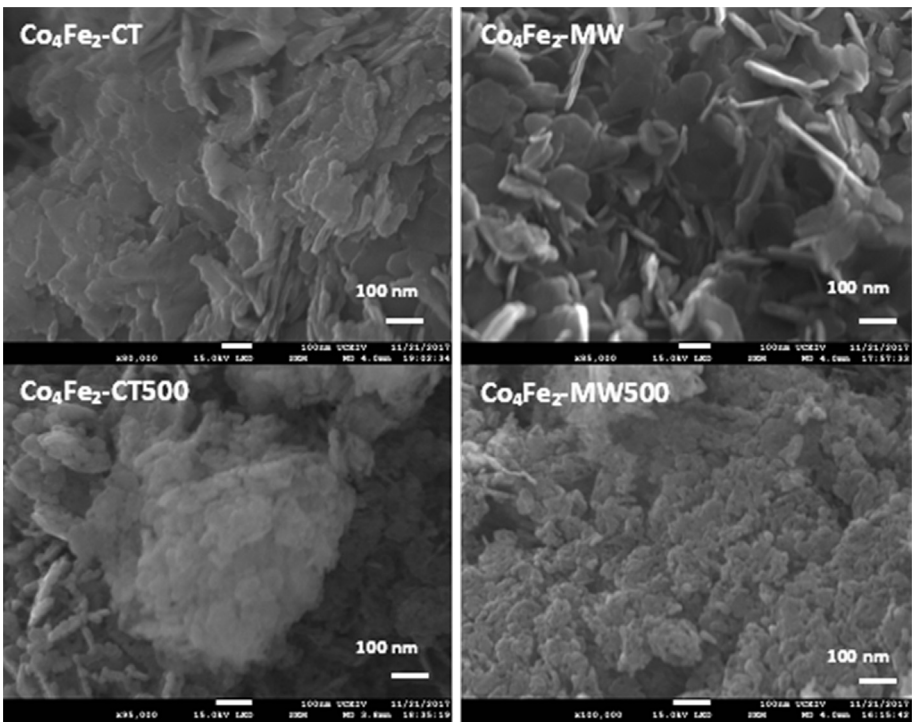

Fig. 4. SEM images of the Co_4Fe_2 samples.

3.2. Catalytic performance

Fig. 5(a) displays the evolution of propene conversion to CO_2 versus the reaction temperature for the different prepared catalysts. In fact, propene is a harmful alkene with high photochemical ozone creation potential [24]. The effects of internal diffusions were eliminated by using particle sizes between 500 and 355 μm for all samples at the same reaction conditions. For all catalysts, only CO_2 was detected as a product. The light-off curves of the series of samples exposed to microwave irradiation shifted remarkably to lower temperatures. According to T_{50} values (temperature at which 50 % of propene is converted into CO_2) listed in Table 2, the catalytic performance can be established in the following order: Co_4Fe_2-MW500 > Co_4Al_2-MW500 > Co_4Fe_2-CT500 > Co_4Al_2-CT500 > Mg_4Fe_2-MW500 > Mg_4Fe_2-CT500 > Mg_4Al_2-MW500 > Mg_4Al_2-CT500. Comparing T_{50} of conventional and microwave treated catalysts, a difference of 30 °C is noticed between Co_4Fe_2-CT500 and Co_4Fe_2-MW500 as well as between Co_4Al_2-CT500 and Co_4Al_2-MW500. The enhancement is significantly shown with Mg_4Al_2 solid, where Mg_4Al_2-CT500 catalyst is considerably less active than Mg_4Al_2-MW500. This efficient catalytic activity after microwave irradiation can be attributed to the fact that Mg_4Al_2-MW500 sample has a higher surface area according to BET measurement, a lower crystallite size, and higher pore diameter.

Noteworthy, even when the catalyst Co_4Fe_2 was submitted to 45 and 10 s of irradiation, better catalytic activities toward the total oxidation of propene were obtained as compared with the conventional Co_4Fe_2-CT500 catalyst (Fig. 5(b)). Catalytic activities of Co_4Fe_2 catalysts were evaluated at 20 % of propene conversion and are presented in Table 3. There is a correlation for all Co-Fe–containing samples between the catalytic activity and the microwave irradiation time. Co_4Fe_2-CT500 exhibits the lowest catalytic

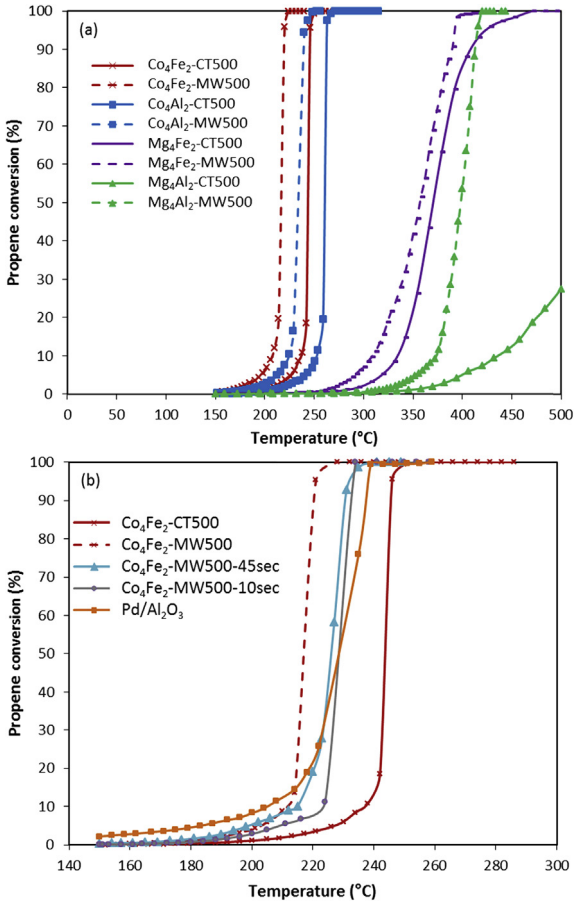

Fig. 5. Propene conversion to CO_2 vs reaction temperature for the samples (a) prepared via the hydrotalcite route and microwave irradiations; (b) Pd/Al_2O_3 and Co_4Fe_2 treated under microwave irradiation at a fixed power of 40 W for different durations.

Table 3
Surface area, total H_2 consumption, temperature (T_{20}), and catalytic activity of 20 % of propene conversion for the different cobalt iron-based catalysts.

Samples	Surface area ($m^2\ g^{-1}$)	Total H_2 consumption (μmol g^{-1})	T_{20} (°C)	Catalytic activity (mol $h^{-1}\ g^{-1}$)
Co_4Fe_2-CT500	57	16,622	242	0.171
Co_4Fe_2-MW500-10sec	68	17,723	225	0.176
Co_4Fe_2-MW500-45sec	74	17,968	220	0.177
Co_4Fe_2-MW500	80	18,329	215	0.180

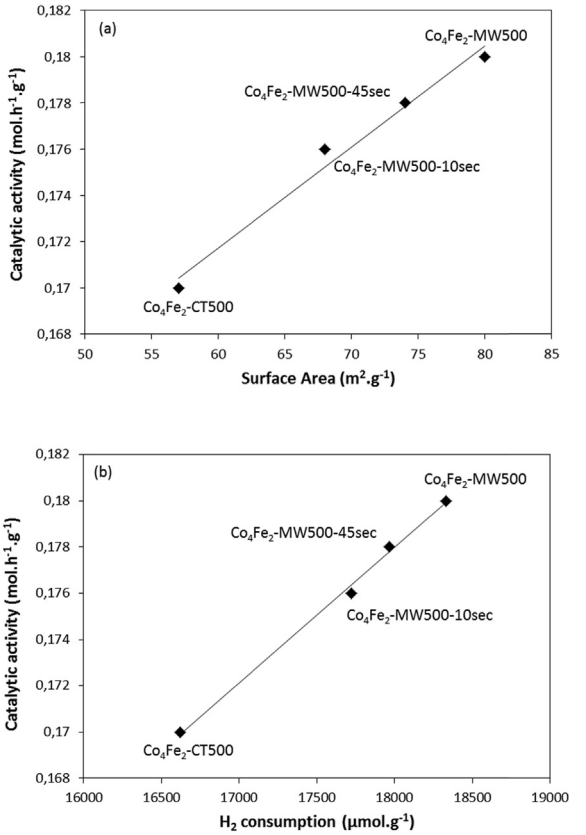

Fig. 6. Influence of (a) the surface area and the (b) H_2 consumption of the different cobalt iron–based catalysts on the catalytic activity at 20 %.

activity. The samples treated under microwave irradiations show higher values. The more the irradiation is longer the more the catalytic activity is higher. Indeed, the better activity can be related to a larger surface area and greater availability of the active phase as shown in Fig. 6(a) and (b). It should be noted that increasing the time of irradiation more than a minute does not give any enhancement in the catalytic activity.

Moreover, it was revealed that Co_4Fe_2 catalysts treated under microwave irradiation oxidizes propene at lower temperatures than a conventional industrial 0.5 wt% Pd/Al_2O_3 catalyst with an expensive noble metal (Fig. 5(b)). A minimum power of 40 W for 1 min, used in this study, was enough to improve the catalytic activity. The total oxidation of propene on hydrotalcite materials could be significantly improved by the microwave irradiation of hydrotalcite [14,20]. Interestingly, even the supported noble metal, Au/Al_2O_3 ($T_{50} = 360$ °C) and Au/xCeO$_2$-Al_2O_3 (T_{50} between 265 and 235 °C) catalysts present lower activities than those found in this study for Co_4Fe_2-MW500 ($T_{50} = 214$ °C) [25]. This result confirms that propene oxidation can take place at a very low temperature with microwave treatment. The advantage of this treatment was not only a significant enhancement of catalytic performance but also a reduction in manipulation time (from 24 h to 1 min) and therefore an energy saving process.

4. Conclusions

Mg-Co/Al-Fe layered double hydroxides were successfully synthesized using a microwave-assisted method. This study shows for the first time that a microwave treatment can be used at a minimum power (40 W) with a minimum irradiation time (1 min) to obtain the hydrotalcite structure. Microwave irradiation led to higher values of specific surface areas and pore diameter. The catalyst preparation using microwave irradiation leads to an open hydrotalcite structure and calcined samples show an improvement in the catalytic activity toward the total oxidation of propene. Moreover, correlations between the catalytic activity and the surface area as well as the H_2 consumption of cobalt iron–based catalysts were obtained. Furthermore, this catalytic activity was improved by increasing the time under microwave irradiation from 10 s to 1 min. Hence, besides this enhancement, the interesting advantage of the microwave treatment is the reduction in manipulation time and power, and therefore a decrease in energy consumption.

Acknowledgments

The "Université du Littoral-Côte d'Opale" (ULCO, France) and the Lebanese University (UL, Lebanon) are gratefully acknowledged for financial supports. The authors would like to thank the "Agence universitaire de la Francophonie—Région du Moyen-Orient" (AUF) and the ULCO for research fellowship. The Interreg V project “DepollutAir” (France, Wallonie, Flandres) funded by the European Union is also gratefully acknowledged for financial support. The authors would also like to thank Karine Deboudt and Xavier Secordel for SEM analysis.

Appendix A. Supplementary data

Supplementary data to this article can be found online at https://doi.org/10.1016/j.crci.2018.09.012.

References

[1] M. Gabrovska, R. Edreva-Kardjieva, D. Crişan, P. Tzvetkov, M. Shopska, I. Shtereva, React. Kinet. Mech. Catal. 105 (2012) 79–99.
[2] P. Li, C. He, J. Cheng, C.Y. Ma, B.J. Dou, Z.P. Hao, Appl. Catal. B 101 (2011) 570–579.
[3] G. Fetter, F. Hernandez, A.M. Maubert, V. Lara, P. Bosch, J. Porous Mater. 4 (1997) 27–30.
[4] Z. Jubri, M.Z. Hussein, A. Yahaya, Z. Zainal, Nanosci. Methods 1 (2012) 152–163.
[5] U. Costantino, F. Marmottini, M. Nocchetti, R. Vivan, Eur. J. Inorg. Chem. 10 (1998) 1439–1446.
[6] K.J. Rao, B. Vaidhyanathan, M. Ganguli, P.A. Ramakrishnan, Chem. Mater. 11 (1999) 882–895.
[7] S.A. Galema, Chem. Soc. Rev. 26 (1997) 233–238.
[8] P. Benito, F.M. Labajos, J. Rocha, V. Rives, Microporous Mesoporous Mater. 94 (2006) 148–158.
[9] P. Benito, I. Guinea, F.M. Labajos, V. Rives, J. Solid State Chem. 181 (2008) 987–996.
[10] O. Bergadà, P. Salagre, Y. Cesteros, F. Medina, J.E. Sueiras, Appl. Catal. A Gen. 331 (2007) 19–25.
[11] O. Bergadà, I. Vicente, P. Salagre, Y. Cesteros, F. Medina, J.E. Sueiras, Microporous Mesoporous Mater. 101 (2007) 363–373.
[12] E. Genty, J. Brunet, C. Poupin, S. Casale, S. Capelle, P. Massiani, S. Siffert, R. Cousin, Catalysts 5 (2015) 851–867.
[13] C. Gennequin, S. Kouassi, L. Tidahy, R. Cousin, J.F. Lamonier, G. Garçon, P. Shirali, F. Cazier, A. Aboukaïs, S. Siffert, C. R. Chimie 13 (2010) 494–501.
[14] R. Mrad, R. Cousin, C. Poupin, A. Aboukaïs, S. Siffert, Catal. Today 257 (2015) 98–103.
[15] F.M. Labajos, V. Rives, M.A.A. Ulibarri, J. Mater. Sci. 27 (1992) 1546–1552.
[16] M. Gabrovska, R. Edreva-Kardjieva, K. Tenchev, P. Tzvetkov, A. Spojakina, L. Petrov, Appl. Catal. A Gen. 399 (2011) 242–251.
[17] S. Kannan, R. Vir Jasra, J. Mater. Chem. 10 (2000) 2311–2314.
[18] J. Jacob, L.H.L.L. Chia, F.Y.C.C. Boey, J. Mater. Sci. 30 (1995) 5321–5327.
[19] E. Genty, R. Cousin, S. Capelle, C. Gennequin, S. Siffert, Eur. J. Inorg. Chem. 16 (2012) 2802–2811.
[20] R. Mrad, R. Cousin, N.A. Saliba, L. Tidahy, S. Siffert, C. R. Chimie 18 (2015) 351–357.
[21] E. Amini, M. Rezaei, M. Sadeghinia, Chin. J. Catal. 34 (2013) 1762–1767.
[22] V. Rives, A. Dubey, S. Kannan, Phys. Chem. Chem. Phys. 3 (2001) 4826–4836.
[23] C.W. Tang, C.B. Wang, S.H. Chien, Thermochim. Acta 473 (2008) 68–73.
[24] R.G. Derwent, M.E. Jenkin, S.M. Saunders, M.J. Pilling, Atmos. Environ. 32 (1998) 2429–2441.
[25] P. Lakshmanan, L. Delannoy, V. Richard, C. Méthivier, C. Potvin, C. Louis, Appl. Catal. B Environ. 96 (2010) 117–125.